JOURNAL OF SYNCHROTRON RADIATION

ISSN 1600-5775

Received 16 November 2016
Accepted 6 April 2017

Edited by S. M. Heald, Argonne National Laboratory, USA

Keywords: time-resolved XAFS; QXAFS; 1W1B; BSRF.

Time-resolved XAFS measurement using quick-scanning techniques at BSRF

Shengqi Chu,[a]* Lirong Zheng,[a] Pengfei An,[a] Hui Gong,[b] Tiandou Hu,[a] Yaning Xie[a] and Jing Zhang[a]*

[a]Multi-Discipline Research Center, Institute of High Energy Physics, Chinese Academy of Sciences, Beijing 100049, People's Republic of China, and [b]Department of Engineering Physics, Tsinghua University, Beijing 100084, People's Republic of China. *Correspondence e-mail: chusq@ihep.ac.cn, jzhang@ihep.ac.cn

A new quick-scanning X-ray absorption fine-structure (QXAFS) system has been established on beamline 1W1B at the Beijing Synchrotron Radiation Facility. As an independent device, the QXAFS system can be employed by other beamlines equipped with a double-crystal monochromator to carry out quick energy scans and data acquisition. Both continuous-scan and trapezoidal-scan modes are available in this system to satisfy the time scale from subsecond (in the X-ray absorption near-edge structure region) to 1 min. Here, the trapezoidal-scan method is presented as being complementary to the continuous-scan method, in order to maintain high energy resolution and good signal-to-noise ratio. The system is demonstrated to be very reliable and has been combined with *in situ* cells to carry out time-resolved XAFS studies.

1. Introduction

Time-resolved X-ray absorption fine structure (XAFS) measurements are essential for investigating *in situ* dynamic processes such as catalysis (Tada *et al.*, 2007; Uemura *et al.*, 2012) and nucleation (Ohyama *et al.*, 2011; Yao *et al.*, 2012). Several techniques have been developed at many synchrotron radiation beamlines to shorten the acquisition time of a full XAFS spectrum down to a few seconds or even milliseconds. Among these, two successful modes are accepted: energy-dispersive geometry (EDXAS) (Matsushita & Phizackerley, 1981; Pascarelli *et al.*, 2006) and quick-scanning acquisition (QXAFS) (Frahm, 1989; Frahm *et al.*, 2005; Richwin *et al.*, 2001; Prestipino *et al.*, 2011; Liu *et al.*, 2012; Mathon *et al.*, 2015; Müller *et al.*, 2016).

The energy-dispersive method can achieve sub-millisecond time resolution by using a polychromatic X-ray beam and recording all data points in one exposure. However, this requires establishing a totally new beamline with complicated and expensive equipment because it is not compatible with conventional beamlines. Besides different optics, EDXAS has extreme requirements for sample homogeneity and difficulty in fluorescence measurements (Prestipino *et al.*, 2011).

QXAFS maintains a full compatibility with the step-by-step mode, based on the double-crystal monochromator (DCM), that is commonly used to perform energy scanning in XAFS experiments. Unlike in the conventional XAFS method, in QXAFS the angle of the crystal monochromator moves continuously and quickly, reducing the collection time of the spectrum drastically from minutes to seconds. It is also very easy to combine with various sample conditions, and thus QXAFS may become the main method in the future with the

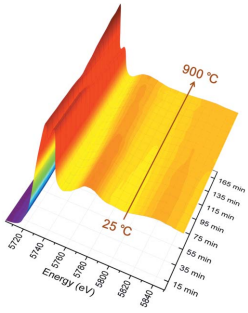

development of advanced photon sources and automatic sample change techniques.

In this paper, we will introduce the QXAFS system built at 1W1B, a general hard X-ray XAFS beamline at Beijing Synchrotron Radiation Facility (BSRF). There are two main advantages of this system: (i) it is programmable, so can control precisely the movement of the Bragg motor in the flying or trapezoidal mode (T-mode), providing the user community with a broad time resolution from subsecond to 1 min; (ii) it is independent and transferable, which means that it can be used immediately by any beamline equipped with a DCM to carry out quick energy scanning and data acquisition. In the next section, a brief introduction of our beamline is given. §3 describes the function and performance of QXAFS. Finally, a time-resolved study is shown in §4.

2. Beamline overview

The 1W1B beamline, located at the Beijing Synchrotron Radiation Facility (BSRF), is dedicated to hard X-ray absorption spectroscopy (XAS) (Xie *et al.*, 2007). BSRF is a first-generation radiation facility; the storage ring supports both high-energy physics experiments (Beijing Electron Positron Collider) and synchrotron radiation research. After an upgrade project in 2008, BSRF now operates in 2.5 GeV full-energy injection and top-up mode with 250 mA beam current in dedicated synchrotron radiation mode. Beamline 1W1B was first open to the user community in 2003. A schematic view of the beamline is shown in Fig. 1. The source is generated by a seven-period permanent-magnet wiggler with a critical energy of 5.32 keV. It is partly cut off by a bend crystal located at 19.8 m from the source, distributing the beam to 1W1A, a diffuse X-ray scattering beamline. The main optical components of beamline 1W1B are a white-beam slit, collimating mirror, fixed-exit Si(111) DCM and toroidal mirror. The incident light from the source is first confined by the white-beam slit in the vertical direction and then focused into a vertical parallel beam by the collimating mirror before reaching the monochromator. The collimating mirror is a meridian focusing silicon mirror coated with 40 nm-thick high-density rhodium, having a 2.6 mrad incident angle and cut-off energy of 25 keV. The Si(111) monochromator is based on a HUBER 420 goniometer with an angular range from 4 to 24°.

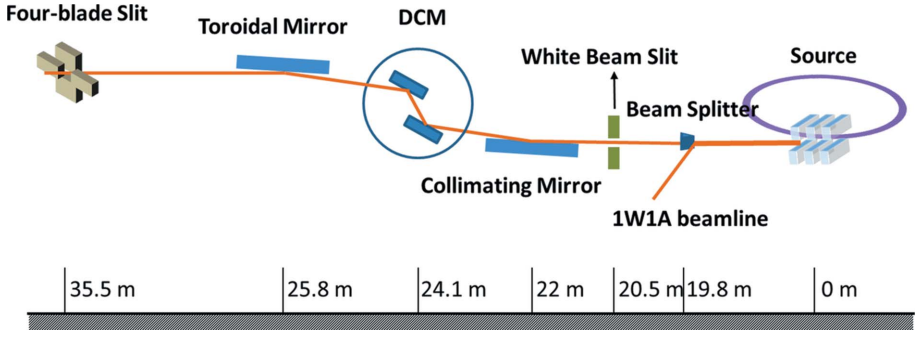

Figure 1
Layout of the key optical components at beamline 1W1B.

Table 1
Major features of the 1W1B beamline.

Storage ring	2.5 GeV, 250 mA
Source	1.28 T, 7 periods wiggler, period length 228 mm
Acceptance angle	1.0 mrad × 0.12 mrad (H × V)
Monochromator	Fixed-exit Si(111) DCM with water cooling
Energy range	4–25 keV
Energy resolution ($\Delta E/E$)	1×10^{-4} to 3×10^{-4}
Flux on sample	$\sim 6 \times 10^{11}$ photons s^{-1} at 10 keV, 200 mA
Beam size on sample	0.9 mm × 0.3 mm (FWHM); 100 µm × 100 µm with polycapillary focusing
Detectors	Ionization chambers, Lytle detector, 19-element high-purity Ge solid-state detector
Established techniques	Transmission and fluorescence modes
	Extreme conditions: low temperature (10 K), high temperature (1300 K), high pressure (50 GPa)
	In situ solid-gas reactor
	Grazing-incidence XAFS method for thin-film samples
	Time-resolved quick-scanning XAFS

A mechanical linkage system is designed to adjust the distance between the two crystals to keep the fixed exit of the outgoing beam (Xie *et al.*, 2001). The second crystal can be finely detuned through an encoder linear actuator to suppress the high harmonics. The monochromatic X-ray beam is finally focused by the toroidal mirror onto the sample, which is also a silicon mirror coated with 40 nm-thick rhodium. A four-blade slit is mounted behind the Be-window exit in order to trim the final beam, stop the stray radiation, and also eliminate small beam movements during the XAFS experiments. The main characteristics of the beamline are listed in Table 1.

3. QXAFS system and performance

For time-resolved XAFS experiments, QXAFS usually converts the motion mechanism of the monochromator (Richwin *et al.*, 2001; Frahm *et al.*, 2005; Müller *et al.*, 2016) or improves the data acquisition system (Prestipino *et al.*, 2011; Liu *et al.*, 2012). The 1W1B beamline has been equipped with a fixed-exit Si(111) DCM. The angle position is rotated through a stepper motor and recorded by an encoder. Ionization chambers (ICs) are used to measure the incident and absorbed X-ray intensity in transmission mode. Using these typical devices, we want to develop such a QXAFS system in order to test how fast it could go.

Our QXAFS system is an independent system that uses a field programmable gate array (FPGA) module as a key logic unit to control the movement of the Bragg motor and data acquisition; thus it is more convenient and portable compared with previous complex acquisition systems for QXAFS (Prestipino *et al.*, 2011; Liu *et al.*, 2012). Generally, the XAFS experiments are carried out in a stepwise manner, *i.e.* waiting for the monochromator mechanics to move and settle, reading

the energy position, collecting the data, and then moving to the next point. A fraction of time is needed for readout of the different devices involved and the communication between them, such as PM16C stepping motor controllers, encoders and analog-to-digital converters (ADCs) or voltage-to-frequency converters (VFCs). Our QXAFS system has combined these functions and can be programmed by FPGA. The advantages of doing so are perfect time synchronization (*i.e.* when to move the energy position and when to collect the data) and no need to wait for responses of other devices, thus improving the time resolution greatly. The FPGA module is beneficial for programming the pulse sequence to achieve continuous- or trapezoidal-scan mode (Fig. 2*a*). During an energy scan, the monochromator position is linear with the number of pulses sent to the Bragg motor, if lost steps and mechanical backlash are not considered. Fortunately, the lost steps can be negligible when the motor speed is under a maximum (in our case, 0.16° s^{-1}), and the backlash is tested to be constant over the whole energy range (in our case, about 190 pulses), which can be compensated for when the scan direction is changed. Further avoiding the effect of backlash, we use the angular position at the end of each scan as a reference to determine the energy axis. Accordingly, the energy difference of repeated measurements in a QXAFS scan is reduced to less than 0.1 eV, and also between QXAFS and step-by-step scans. The XAFS signal can be obtained during both upward and downward scans *via* three-channel parallel acquisition, available for voltage signals by ADCs and pulse counts from VFCs, respectively. The ADCs have a resolution of 14-bits and a sample rate of 80 MHz. In order to be compatible with the conventional mode, three other channels of pulse counter with 100 MHz input count rate are also embedded in the system. All six channels are sampled synchronously. Considering the signal-to-noise ratio (SNR) of the data and limited response time of the parallel-plate IC, the collection time per data point is set to be >1 ms. Fig. 2(*b*) shows a schematic map of the QXAFS measurement. The system can keep running for 10 h without any fault, verifying its stability and repeatability.

By continuously scanning the motor at maximum speed, the acquisition time can be reduced greatly. XANES spectra can be obtained in less than 1 s (Fig. 3), and full EXAFS at the Cu *K*-edge will take about 8 s. Actually, this time resolution of our QXAFS is currently limited by the available maximum rotation speed of the Bragg motor (only 0.16° s^{-1}), beyond which step throwing will occur. It is obvious that the acquisition time will reduce further if the motor can go faster.

Unlike the continuous-scan mode, the T-mode is designed in this system, and similar to the conventional step-by-step mode but accomplished in one take, including the real-time control of motor and sampling. In T-mode, the motor scans quickly but stops or moves at a very low velocity when recording the data (Fig. 2*a*), in order to maintain the high energy resolution and good SNR of the data. As is known, the

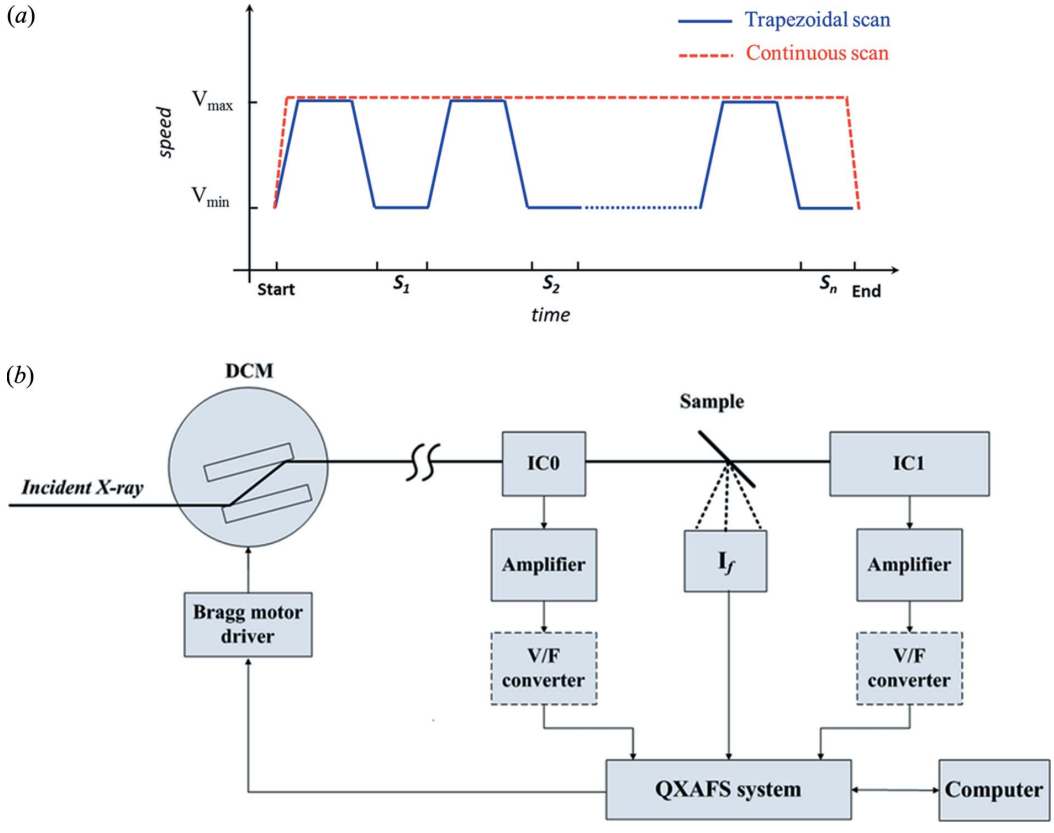

Figure 2
(*a*) Illustration of motor speed and sampling sections (S_1, $S_2 \ldots S_n$) with time in T-mode and continuous-scan mode. (*b*) Schematic diagram of the QXAFS measurement system.

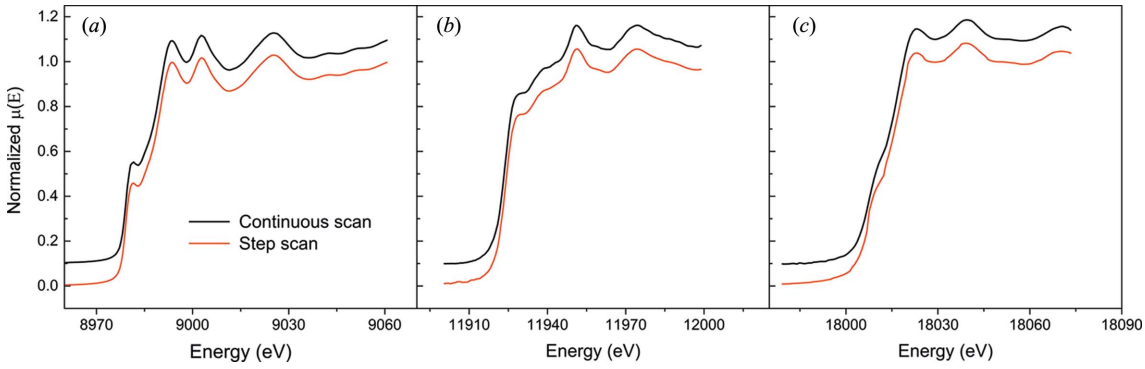

Figure 3
Normalized XANES spectra of (*a*) Cu, (*b*) Au and (*c*) Zr metal foils. The top black lines are for collection by continuous scan in about 1 s at the Cu *K*-edge, 0.6 s at the Au L_3-edge and 0.4 s at the Zr *K*-edge, respectively. The conventional step scan results are also shown as red lines for comparison.

energy resolution will drop during a rapid scan unless a sufficient sampling speed (oversampling) is reached (Liu *et al.*, 2012; Müller *et al.*, 2016). Sometimes the SNR of the data needs to be optimized, by reducing the moving speed of the motor in continuous-scan mode, whereas in T-mode the motor can still be rotated at maximum speed with acceleration and deceleration sections to extremely compress the scanning time. Also, it is easy to vary the sampling time of each energy point from 1 ms to 1 s in T-mode in order to obtain a high-quality spectrum without loss of energy resolution, especially for very complex or diluted samples. Overall, the T-mode has a median time resolution of tens of seconds to one or two minutes. As an important complement to the continuous scan, it can be applied to some slow processes taking one or two hours (Yao *et al.*, 2012).

The *K*-edge of copper standard foil was measured with a post-edge range up to 1000 eV by trapezoidal scan. As shown in Fig. 4, the result, which was collected in about 17 s, kept the same energy resolution in the near-edge region and good SNR at the high-*k* part compared with the step-by-step mode, which took 15 min. In view of the efficiency, it is likely to replace the conventional collection method in the future. The results of continuous QXAFS are also shown in Fig. 4 for comparison. Very little difference is found between the three modes, proving the reliability of our QXAFS system.

4. Applications

To test the performance, the structural origin of oxygen storage and release in ceria nanocrystals was investigated by the QXAFS system. The sample was heated up to 900°C in an *in situ* cell at a rate of 5°C min^{-1} (An *et al.*, 2014), while the Ce L_3-edge XANES spectra were collected simultaneously at 32 s per scan in T-mode. In Fig. 5, it can be clearly seen that the Ce oxidation state varied from +4 (CeO_2) to +3 (Ce_2O_3), which was coupled with oxygen-vacancy formation and migration. This dynamic process is crucial for figuring out the microscopic mechanism of ceria for storing, releasing and transporting oxygen (Zhang *et al.*, 2001; Skorodumova *et al.*, 2002).

5. Conclusion

A QXAFS system has been developed at beamline 1W1B at BSRF. This system is independent and is fully compatible with the step-by-step mode, so it is easy to use on other general

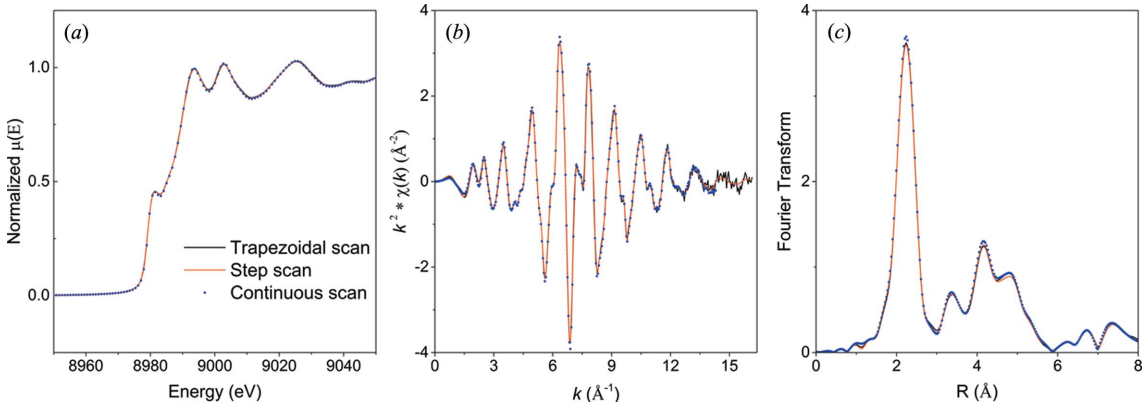

Figure 4
Comparison of XAFS spectra collected using QXAFS by trapezoidal scan (black solid line), step-by-step method (red solid line) and continuous scan (blue marked points) in the (*a*) XANES range, (*b*) *k*-space and (*c*) *R*-space. The *k*-range for Fourier transformation is from 3 to 13.2 $Å^{-1}$ with Hanning window.

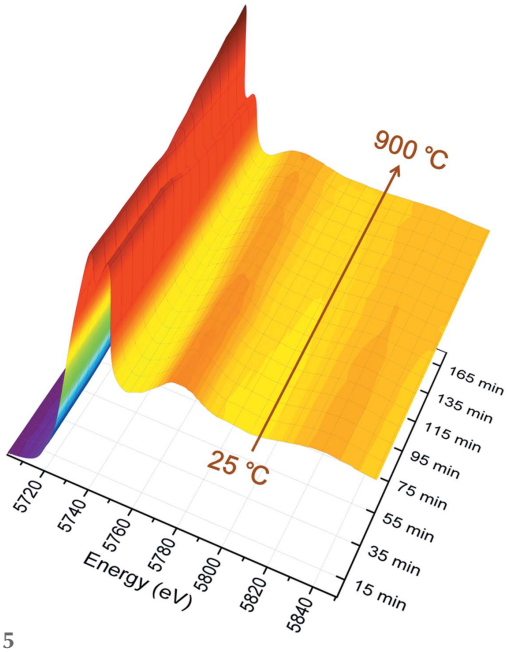

Figure 5
Ce L_3-edge XANES spectra as a function of temperature. Each spectrum was obtained in 32 s using QXAFS by trapezoidal scan.

XAFS beamlines. Based on a FPGA, both the continuous-scan and T-modes are very easy to implement in the system to cover a broad time resolution from subsecond to 1 min. Actually, the time-resolved ability is now limited by the maximum speed of the Bragg motor, not the system itself. The system runs well and has provided the user community with the ability to perform *in situ* XAFS experiments.

Acknowledgements

This work was financially supported by the National Natural Science Foundation of China (Grant No. 11305109, 11135008, 11375229).

References

An, P., Hong, C., Zhang, J., Xu, W. & Hu, T. (2014). *J. Synchrotron Rad.* **21**, 165–169.
Frahm, R. (1989). *Rev. Sci. Instrum.* **60**, 2515–2518.
Frahm, R., Richwin, M. & LtzenkirchenHecht, D. (2005). *Phys. Scr.* T**115**, 974–976.
Liu, H., Zhou, Y., Jiang, Z., Gu, S., Wei, X., Huang, Y., Zou, Y. & Xu, H. (2012). *J. Synchrotron Rad.* **19**, 969–975.
Mathon, O., Beteva, A., Borrel, J., Bugnazet, D., Gatla, S., Hino, R., Kantor, I., Mairs, T., Munoz, M., Pasternak, S., Perrin, F. & Pascarelli, S. (2015). *J. Synchrotron Rad.* **22**, 1548–1554.
Matsushita, T. & Phizackerley, R. P. (1981). *Jpn. J. Appl. Phys.* **20**, 2223–2228.
Müller, O., Nachtegaal, M., Just, J., Lützenkirchen-Hecht, D. & Frahm, R. (2016). *J. Synchrotron Rad.* **23**, 260–266.
Ohyama, J., Teramura, K., Higuchi, Y., Shishido, T., Hitomi, Y., Aoki, K., Funabiki, T., Kodera, M., Kato, K., Tanida, H., Uruga, T. & Tanaka, T. (2011). *Phys. Chem. Chem. Phys.* **13**, 11128–11135.
Pascarelli, S., Mathon, O., Muñoz, M., Mairs, T. & Susini, J. (2006). *J. Synchrotron Rad.* **13**, 351–358.
Prestipino, C., Mathon, O., Hino, R., Beteva, A. & Pascarelli, S. (2011). *J. Synchrotron Rad.* **18**, 176–182.
Richwin, M., Zaeper, R., Lützenkirchen-Hecht, D. & Frahm, R. (2001). *J. Synchrotron Rad.* **8**, 354–356.
Skorodumova, N. V., Simak, S. I., Lundqvist, B. I., Abrikosov, I. A. & Johansson, B. (2002). *Phys. Rev. Lett.* **89**, 166601.
Tada, M., Murata, S., Asakoka, T., Hiroshima, K., Okumura, K., Tanida, H., Uruga, T., Nakanishi, H., Matsumoto, S., Inada, Y., Nomura, M. & Iwasawa, Y. (2007). *Angew. Chem. Int. Ed.* **46**, 4310–4315.
Uemura, Y., Inada, Y., Niwa, Y., Kimura, M., Bando, K. K., Yagishita, A., Iwasawa, Y. & Nomura, M. (2012). *Phys. Chem. Chem. Phys.* **14**, 2152–2158.
Xie, Y. N., Hu, T. D., Liu, T. & Zhang, J. (2007). *AIP Conf. Proc.* **879**, 856–859.
Xie, Y. N., Yan, Y., Hu, T. D., Liu, T. & Xian, D. C. (2001). *Nucl. Instrum. Methods Phys. Res. A*, **467–468**, 748–751.
Yao, T., Liu, S., Sun, Z., Li, Y., He, S., Cheng, H., Xie, Y., Liu, Q., Jiang, Y., Wu, Z., Pan, Z., Yan, W. & Wei, S. (2012). *J. Am. Chem. Soc.* **134**, 9410–9416.
Zhang, J., Wu, Z., Liu, T., Hu, T., Wu, Z. & Ju, X. (2001). *J. Synchrotron Rad.* **8**, 531–532.